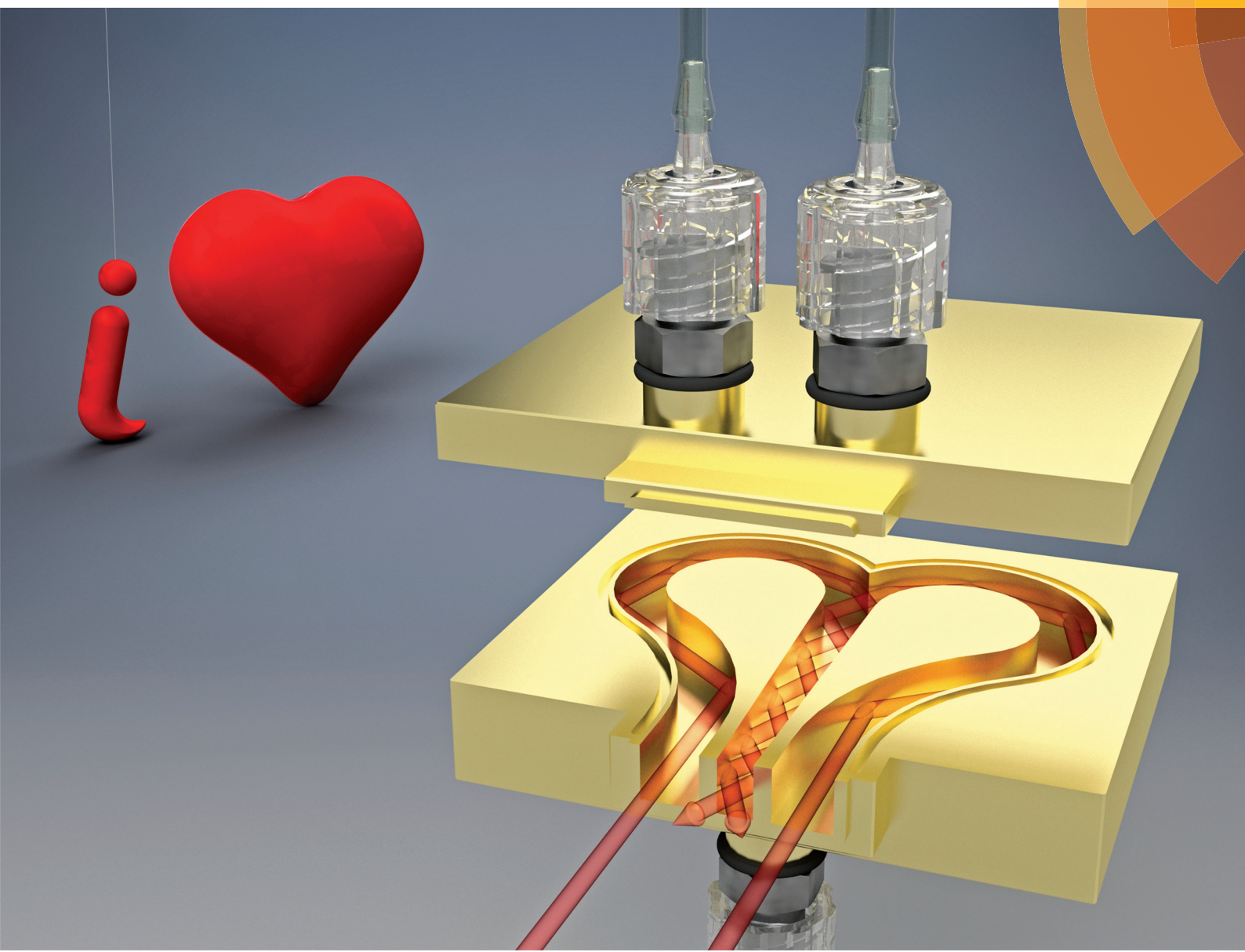
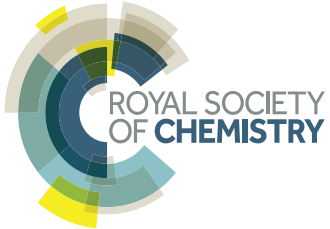


Analyst

www.rsc.org/analyst



ISSN 0003-2654



PAPER

Ivo M. Raimundo Jr., Boris Mizaikoff *et al.*

iHEART: a miniaturized near-infrared in-line gas sensor using heart-shaped substrate-integrated hollow waveguides

175 YEARS



Cite this: *Analyst*, 2016, **141**, 5298

iHEART: a miniaturized near-infrared in-line gas sensor using heart-shaped substrate-integrated hollow waveguides

Rafael L. Ribessi,^a Thiago de A. Neves,^a Jarbas J. R. Rohwedder,^a Celio Pasquini,^a Ivo M. Raimundo, Jr.,^{*a} Andreas Wilk,^b Vjekoslav Kokoric^b and Boris Mizaikoff^{*b}

A novel heart-shaped substrate-integrated hollow waveguide (hiHWG) was integrated with a near-infrared micro-spectrometer (μ NIR) for sensing natural gases, resulting in an ultra-compact near-infrared gas sensing system – iHEART. The iHEART system was evaluated using two different μ NIR spectrometers, and the performance was compared with a laboratory NIR spectrometer for gas analysis based on an acousto-optic tunable filter (AOTF). The spectral data were pre-processed using the 1st derivative Savitzky–Golay algorithm, and then used for establishing multivariate regression models based on partial least squares (PLS). The root mean square errors of prediction (RMSEPs) obtained for major components of natural gas with both iHEART systems were similar to those associated with the AOTF spectrophotometer combined with a conventional long-path measurement cell. It was demonstrated that the iHEART system has significant potential for the development of compact in-line gas sensing systems, thus facilitating monitoring of (petro)chemically relevant processes and products. However, the flexibility and modularity of the system also allows tailoring iHEART to a wide range of other relevant analytical measurement scenarios requiring short response times and minute gas sample volumes.

Received 3rd May 2016,
Accepted 31st July 2016

DOI: 10.1039/c6an01027j

www.rsc.org/analyst

Introduction

In recent years, the field of analytical chemistry is experiencing a rapid improvement in analytical techniques with major attention to novel instrumentation, sensors, and systems. A distinct trend in analytical instrumentation is the emergence of increasingly compact devices that allow precise and accurate acquisition of data in real-time on location.¹ Technological advancements in the areas of new materials, optics, and electronics are particularly paving the way for the development of robust optical and spectroscopic sensing systems. Nowadays, a wide variety of portable instruments based on UV-Vis,² Raman,³ X-ray,⁴ and mid-infrared (MIR)⁵ as well as near-infrared (NIR)⁶ spectroscopy are routinely applied in industrial process control, environmental monitoring and medical/clinical analysis.

The development of advanced systems for *in situ* applications remains one of the most significant challenges in analytical instrumentation because of the demanded simplification and miniaturization, yet maintaining acceptable

analytical-figures-of-merit when addressing relevant analytical scenarios under in-field conditions. Basic attributes, such as small dimension and weight, power autonomy, robustness, and sophisticated calibration and data evaluation routines rapidly providing analytical results at varying environmental conditions are desired.⁷ Regarding size and weight, analyzers are conventionally classified into transportable systems (>10 kg), portable systems (<10 kg), and hand-held devices (<0.5 kg).⁷

A relatively new optical analyzer platform with suitable characteristics for in-field applications are ultra-compact NIR spectrometers (in the present study, μ NIR by Viavi, Milpitas, CA, USA), which operate in the 900–2500 nm wavelength band.⁸ Usually, spectral measurements are executed either in diffuse reflectance or in transmittance mode. Such portable self-containing instruments (*i.e.*, comprising radiation source and detector) are highly miniaturized, weighing approx. 70 g, do not contain any moving component, and use monochromators based on thin-film Fabry-Perot cavities with variable thickness or interference filters.⁸ After selection of specific or narrow ranges of wavelengths, the signal is projected onto a detector array located immediately after the filter wedge, thereby providing immediate access to the entire NIR spectrum. With this simple design, the μ NIR has been demonstrated as an effective tool for analyzing solids,^{8,9} liquids,^{10,11}

^aInstitute of Chemistry, University of Campinas, 13083-970 Campinas, Brazil.

E-mail: ivo@iqm.unicamp.br

^bInstitute of Analytical and Bioanalytical Chemistry, Ulm University, Albert-Einstein-Allee 11, 89081 Ulm, Germany. E-mail: boris.mizaikoff@uni-ulm.de



and gases.¹² For liquid samples, two strategies have been used based on transmittance and transfectance measurements. In the first approach, an external light source powered *via* the USB port of a notebook and a liquid cell with an optical path length of 20 mm were employed for the determination of biodiesel in diesel/biodiesel blends, and for identifying adulteration by vegetable oil.¹⁰ In the latter strategy, a spherical gold mirror was coupled to the μ NIR spectrometer, and transfectance measurements were performed using a cuvette with an optical path length of 1 mm to determine ethanol in gasoline.¹¹

A recent application by our research team revealed the fundamental potential of this system serving as an analyzer for the quantification of natural gas mixtures using multivariate regression models.¹² Natural gas is a relevant matrix in fuel and petrochemical industries. While the feasibility of this sensing concept was fundamentally shown, some major limitations were encountered due to the geometry of a conventional substrate-integrated hollow waveguide (iHWG), which required an external radiation source just taking advantage of the dispersive component and the detector of the μ NIR. iHWGs have been pioneered by the Mizaikoff research team, and represent the current state-of-the-art in hollow waveguide structures that simultaneously act as a photon conduit – from the UV to THz wavelengths – and as a highly miniaturized gas cell characterized by minute sampling volumes, rapid sample transients, and short response times.^{12–16}

The iHEART system shown herein evolves the μ NIR based sensing unit into the first prototype of a portable NIR gas sensor system by combination with a novel heart-shaped substrate-integrated hollow waveguide (hiHWG), specifically tailored to the optical arrangement of the μ NIR.³ The hiHWG enables using both radiation sources integrated into the μ NIR, thereby facilitating a fully integrated system design. The iHEART system was evaluated for quantifying the major constituents in natural gas by coupling two μ NIR spectrometers operating in different wavelength regimes (915–1650 nm and 1150–2150 nm). The results were compared to a laboratory NIR spectrometer based on an acousto-optic tunable filter (AOTF) operating in the 1500–2750 nm regime coupled to a conventional long-path gas cell.

Experimental

Materials and methods

High purity gases (methane (99.95%), ethane (99.95%), propane (99.95%), and butane (99.95%)) supplied by White Martins (Campinas, Brazil) were used for the preparation of gas mixtures. Gas mixtures were prepared by merging individual gas streams controlled *via* flowmeters (Aalborg, New York, USA) that had been previously calibrated using a bubble meter. Each gas flow rate was independently controlled, thereby enabling mixing *via* the volumetric percentage of each gas within the mixture gas stream. The mixtures prepared for establishing the multivariate calibration were selected based

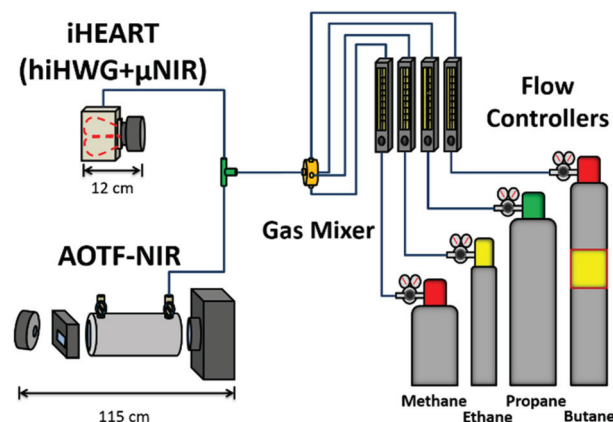


Fig. 1 Scheme of the experimental setup used for analyzing natural gas mixtures evaluated by the iHEART sensor and the AOTF–NIR system. Red dashed lines indicate the heart-shaped waveguide structure of the hiHWG.

on the concentrations of these hydrocarbons found in natural gases, considering independent variations in their concentrations to minimize internal correlations. Consequently, seventy mixtures were prepared with the concentration of each gas varied as follows: 30–90% for methane, 10–50% for ethane, 3–30% for propane, and 0.8–20% for butane, according to their occurrence in natural gas. Gas chromatography coupled with mass spectrometry (GC-MS) was used to evaluate the repeatability of the gas-mixture preparation procedure, and to determine the correct concentration of each gas in the mixtures for providing validated concentration values. Fig. 1 shows the experimental setup to perform measurements with iHEART and AOTF spectrophotometric systems.

GC-MS measurements

All gas mixtures were analyzed using a gas chromatograph 17A coupled to a mass spectrometer QP5050A (Shimadzu, Kyoto, Japan) to evaluate the repeatability and validate the composition of the gas mixtures. A capillary column TG-BOND Q (Thermo Scientific, Waltham, USA) with a length of 30 m, an internal diameter of 0.32 mm, and a stationary phase film thickness of 10 μ m was employed. The carrier gas was helium at a flow rate of 2.5 mL min^{−1}. The samples were manually injected using Hamilton (Reno, USA) gastight syringes. The injection volume was 100 μ L per sample in split mode (1 : 100). An isotherm of 35 °C (held 1 min) up to 150 °C at increments of 40 °C min^{−1} (held 2 min) was used for gas separation in the analytical column. The mass range from m/z = 12 to m/z = 60 was used for establishing the analytical parameters for each analyzed gas sample.

μ NIR spectrometer

Two μ NIR spectrometers, named μ NIR 1700 and μ NIR 2200 (Viavi, Milpitas, CA, USA) operating in different wavelength regimes, were employed. The μ NIR spectrometers were alternatively coupled to the hiHWG, as shown in Fig. 2. Using the



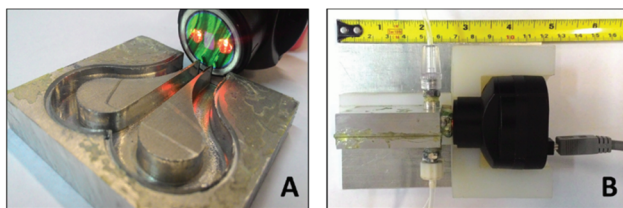


Fig. 2 Images of the hiHWG, showing the heart-shaped optical channels collecting the radiation (red spots) from the μ NIR (A), and of the iHEART, showing the hiHWG directly interfaced with the μ NIR (B).

μ NIR 1700, spectra were collected *via* an integration time of 12 ms by averaging 200 scans (μ NIR system control software version 1.4). For the μ NIR 2200, an integration time of 9 ms and an average of 200 scans were applied (μ NIR system control software version 1.6.1). All measurements were executed keeping the gas mixtures flowing through the hiHWG unit (*i.e.*, continuous flow mode). The precise spectral range captured with the μ NIR 1700 was 909.1–1676.2 nm *vs.* 1558.8–2169.4 nm with the μ NIR 2200.

hiHWG

The general iHWG concept, *i.e.*, the formation of a closed waveguide channel structure by stacking several solid substrate layers, and its specific advantages over the conventional hollow waveguide technology were first described in 2013 by the Mizaikoff group.¹³ Since then, the concept has been successfully applied and tailored to various MIR and NIR gas phase sensing scenarios.^{12,14–16} For the device used in the present study, we have combined NIR radiation emitted from two distinct light sources entailed in the μ NIR spectrometers into a single (centered) output channel illuminating the μ NIR-integrated line array detector *via* providing a tailored heart-shaped iHWG structure. The NIR beams propagate by internal reflections along the polished walls of the waveguide/gas cell conduit. Specifically, waveguide channels with a cross section of 5 mm were milled into a 45 × 50 × 10 mm aluminum alloy base substrate (*cf.* Fig. 2A), and bonded (gas-tight) to a matching top plate polished to a mirror-like surface finish, thus establishing a heart-shaped waveguide (hiHWG) with approx. 4.0 cm^3 volumetric capacity. The top and/or bottom plates feature narrow bore through-holes close to the optical in- and out-coupling facets serving as gas in- and outlets. The waveguide channels were gas-tight butt-coupled against the sapphire window of the μ NIR spectrometer, thereby enabling efficient radiation coupling into the hiHWG, which simultaneously serves as a gas cell.

AOTF-NIR spectrometer

Fig. 3 shows a scheme of the AOTF-NIR spectrometer assembly. From right to left, a tungsten lamp 50 W (Osram, Osasco, Brazil) serving as a radiation source is collimated by a plano-convex lens (CaF_2 ; Ealing, Scotts Valley, USA), and propagates through the gas cell (565 mm optical path, custom-made)

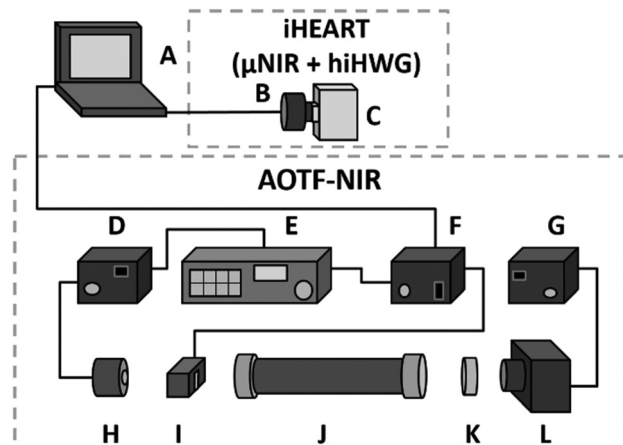


Fig. 3 Schematic of an iHEART sensor and an AOTF–NIR spectrometer. Microcomputer (A), μ NIR (B), hiHWG (C), detector controller (D), amplifier and lock-in filter (E), radio frequency generator (F), power supply for a lamp (G), InAs detector (H), acoustic optical tunable filter (AOTF) (I), gas cell (J), CaF_2 lens (K), and tungsten lamp (L).

sealed with glass windows. Wavelength selection is performed by an acoustic-optical tunable filter (AOTF; model TEAF% – 1.5–3.0 UH, Brimrose, Baltimore, USA), driven by a radio frequency generator (VFI-50-32-SPS-B2-C4, Brimrose, Baltimore, USA). Finally, the thus obtained monochromatic radiation is focused onto a detector (PbS ; Ealing, Scotts Valley, USA). The control software of the instrument was programmed in-house in Visual Basic 6 (Microsoft Corp., Redmond, USA). The spectral window of this system extends from 1500 to 2750 nm; all spectra reported herein represent an average of three scans.

Data treatment

For multivariate data treatment, the software The Unscrambler 10.3 (Camo, Oslo, Norway) was used throughout. The calibration data set comprised 70 mixtures that were divided into two sub-sets *via* the Kennard–Stone algorithm, *i.e.*, 50 samples for calibration and 20 for external validation. The NIR spectra obtained from the μ NIR systems were first smoothed using the Savitzky–Golay algorithm across a 7-point window, 2nd-order polynomial. All data pre-treatments were uniform for both μ NIR systems and the AOTF–NIR system. The spectral data were subject to mean centering, and the 1st derivatives (Savitzky–Golay algorithm, 5 points window, 2nd-order polynomial) were calculated. For the PLS models using spectra obtained from the μ NIR systems, the spectral region selection confined the applied wavelength window to the range with the highest signal-to-noise ratio (*i.e.*, for the μ NIR 1700: 1100.1–1676.2 nm, and for the μ NIR 2200: 1305.5–2169.4 nm). The PLS models based on the spectra acquired from the AOTF–NIR system utilized the entire spectral range. PLS models were then obtained using the NIPALS algorithm to extract the factors, and leave-one-out cross-validation was used for the target gases. The number of factors for each PLS model was automatically optimized for the lowest value of the root



mean square error of prediction (RMSEP), and further evaluated for the actually suitable number of factors during the validation step.

Results and discussion

The μ NIR employed in the present study was selected due to exceptionally suitable characteristics including compactness, portability, and excellent analytical performance, which was evaluated during the previous work of our research team.¹² The iHEART gas sensor was evaluated considering its applicability for determining the composition of natural gases, represented by mixtures of methane, ethane, *n*-propane and *n*-butane. In addition, two different μ NIR spectrometers were coupled to the hiHWG for demonstrating its feasibility of operation throughout the entire NIR spectral range. Fig. 4 shows the spectra of pure *n*-alkanes, obtained from both iHEART systems, as well as from the AOTF-NIR spectrometer. As can be seen, although presenting adequate signal-to-noise ratios (SNRs), spectra of the four hydrocarbons are strongly overlapping, thus demanding appropriate multivariate calibration strategies.

Repeatability and validation of the gas mixtures

GC-MS was used to evaluate the repeatability of the prepared calibration, and sample mixtures were later analyzed *via* iHEART and AOTF-NIR. For deriving the repeatability of the mixture preparation procedure, mixture compositions were randomly selected, prepared, and independently analyzed five times *via* GC-MS. The figures of merit for the GC-MS method are summarized in Table 1. The repeatability was expressed in terms of the coefficient of variation (CV), and was initially determined in the range of 7.4–9.2%. A CV < 10% for gas mixtures prepared using flowmeters and a mixture chamber for homogenizing the gas sample was considered adequate for the purpose of the present study. Considering these results, all calibration and validation sample sets were prepared based on

Table 1 GC-MS figures-of-merit for the determination of natural gas components

	t_R ^a (min)	R^2	LOD ^b (% v/v)	LOQ ^c (% v/v)	CV ^d (%)
Methane	1.20	0.998	3.7	12.4	8.6
Ethane	2.40	0.994	3.4	11.4	7.0
Propane	4.10	0.998	0.3	0.9	9.2
Butane	5.70	0.998	0.9	2.9	7.4

^a Retention time. ^b Limit of detection (3σ). ^c Limit of quantification (10σ). ^d Coefficient of variation indicating the repeatability of preparing standard mixtures using flowmeters ($n = 5$).

the ratios of flowmeters for each gas, without any further confirmation of the respective concentrations by GC-MS.

Multivariate spectral data evaluation

Fig. 5 shows the spectra of the 70 gas mixtures, obtained from the three NIR systems. It can be noted that baseline variations occur and that spectra provided by hiHWG- μ NIR2200 present the least favourable signal-to-noise ratio. In order to circumvent these issues, all obtained data were pre-treated as described in the Experimental section. Fig. 6 exemplifies the effectiveness of data treatment for spectra obtained from the hiHWG- μ NIR2000 system. Similar results were observed for the other two spectral data sets.

The presence of anomalous samples was verified during the construction of PLS models. For this, limit values for leverage and F-residue (with 95% confidence) were calculated for each model and samples that had higher values than these limits for at least one parameter were excluded one by one from the model.¹⁷ Therefore, models were re-calculated and re-evaluated, and if there were some outliers left the process was repeated. Therefore, for PLS models using data obtained from the μ NIR1700, one sample was removed from the methane model, three from the ethane model, one from the propane model, and four from the butane model. For PLS models using the μ NIR2200, two samples were removed from the

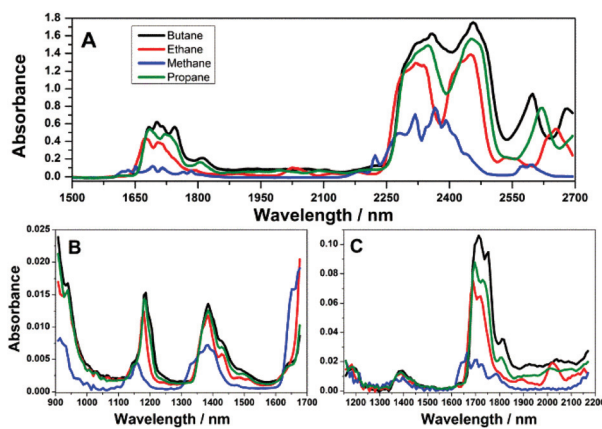


Fig. 4 NIR spectra of pure *n*-alkanes obtained from the AOTF system (A), iHEART- μ NIR1700 (B), and iHEART- μ NIR2200 (C).

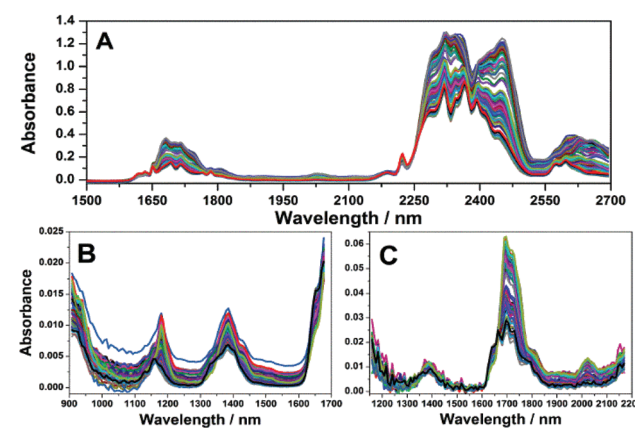


Fig. 5 NIR spectral data set obtained for gaseous mixtures with the AOTF system (A), hiHWG- μ NIR1700 (B), and hiHWG- μ NIR2200 (D).



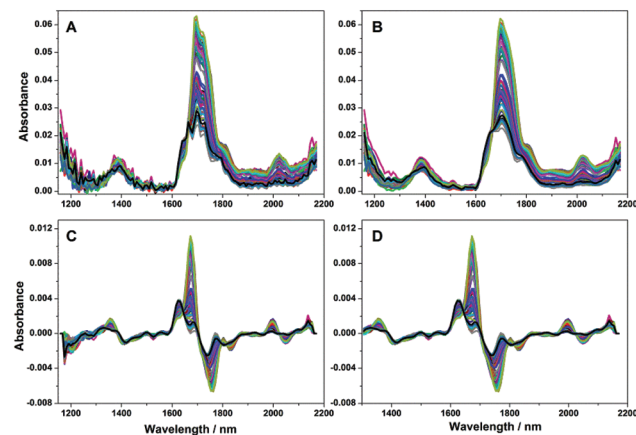


Fig. 6 Effect of data treatment on the collected NIR spectra for iHEART with the μ NIR2200: raw spectra (A), smoothed spectra (b), 1st derivative spectra (C), and spectral region confinement for establishing the multivariate models (D).

butane model. Finally, for PLS models using the AOTF-NIR system, two samples were detected as outliers and removed from the methane model, and two samples were from the butane model. The inclusion of anomalous samples can degrade the performance of the regression model; for example, samples with high leverage values distort the model, making it tendentious and, therefore, generate higher errors in predicted values.¹⁷ Anomalous samples may have been generated by errors in the preparation of mixtures or by some instrumental fluctuation during the measurement.¹⁷

After removing outliers, Kennard–Stone algorithm was employed to select 20 spectra, which were removed from the calibration set and employed for external validation of the models. Table 2 lists the figures of merit provided by PLS models for calibration, cross-validation and external validation for the three systems under consideration, demonstrating the adequate performance of both iHEART systems, compared

to the AOTF-NIR system. Limits of detection and quantification for the multivariate models were calculated *via* eqn (1) and (2):

$$\text{LOD} = 3\sigma_B \|\mathbf{b}\| \quad (1)$$

$$\text{LOQ} = 10\sigma_B \|\mathbf{b}\| \quad (2)$$

where $\|\mathbf{b}\|$ is the norm of the regression vector, and σ_B is the standard deviation of the background.^{17,18} The LOD and LOQ values determined for the AOTF system are evidently superior to the sensing devices due to the extended optical path length *vs.* the hiHWG. In addition, the 1500–2700 nm region in which the AOTF operates covers the regime of combination and the first overtone bands, which present the highest intensities in the NIR spectrum. Likewise, the LOD and LOQ values for propane and butane obtained *via* the μ NIR-1700 are higher compared to the μ NIR-2200, because the 900–1700 nm region encompasses the third and second overtone bands, which are evidently less intense than the first overtone bands at 1700–2150 nm.

Fischer's test was used to assess whether the deviations obtained from the investigated systems are significant at a confidence level of 95%.^{17,18} Comparing both iHEART systems with the AOTF-NIR it was evident that the obtained results for the predictive models of methane and ethane were statistically similar for all systems. However, for the other gases only both iHEART systems appear similar. The performance of the AOTF-NIR system is superior for propane and butane, as this system takes the advantage of a longer optical path in the determination of less concentrated analytes. Furthermore, it was investigated whether systematic errors are present within the developed multivariate models using the t_{bias} -test,¹⁸ again at a level of 95% confidence. The t_{bias} value is calculated for each model, based on its bias, standard deviation and number of samples of the external validation set.¹⁸ All calculated t_{bias} values for validation were lower than the tabulated t_{critical} values, which demonstrates that the models do not present any significant inherent systematic errors as applied herein.

Table 2 Figures of merit for calibration, cross-validation and prediction for the four gases in the three systems

Gas (conc. range)	System	Factor	LOD (%)	LOQ (%)	Calibration		Cross validation		External validation	
					RMSEC (%)	R^2	RMSECV (%)	R^2	RMSEP (%)	R^2
Methane (30–90%)	AOTF	4	0.03	0.09	0.785	0.998	0.917	0.998	0.747	0.998
	μ NIR-1700	3	0.42	1.41	1.156	0.997	1.334	0.996	0.772	0.997
	μ NIR-2200	4	0.49	1.62	0.680	0.999	1.044	0.997	0.804	0.998
Ethane (10–50%)	AOTF	4	0.02	0.08	0.570	0.998	0.667	0.998	0.620	0.998
	μ NIR-1700	3	0.59	1.96	0.659	0.998	0.805	0.997	0.750	0.912
	μ NIR-2200	4	0.58	1.93	0.623	0.998	0.973	0.995	0.772	0.997
Propane (3–30%)	AOTF	4	0.03	0.08	0.346	0.998	0.405	0.997	0.397	0.999
	μ NIR-1700	4	1.42	4.74	0.985	0.982	1.230	0.973	1.030	0.912
	μ NIR-2200	3	0.82	2.74	0.961	0.984	1.232	0.975	1.098	0.939
Butane (0.8–20%)	AOTF	4	0.02	0.08	0.208	0.998	0.250	0.997	0.301	0.963
	μ NIR-1700	5	1.67	5.55	0.726	0.975	0.976	0.957	0.540	0.985
	μ NIR-2200	5	0.73	2.42	0.523	0.987	0.846	0.967	0.797	0.942



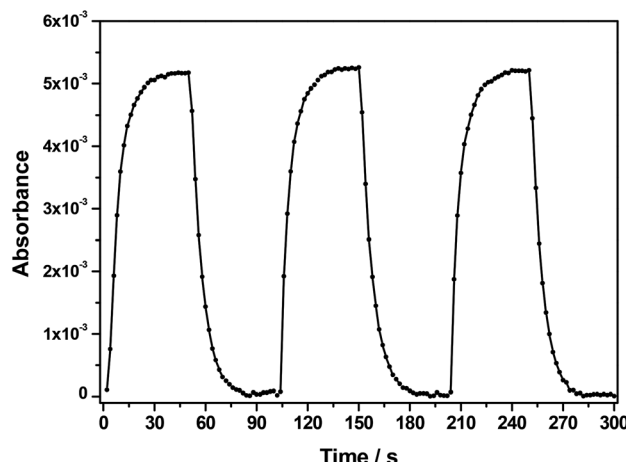


Fig. 7 Response time of the iHEART sensor for methane (flow rate 280 mL min^{-1}) and for purging with nitrogen (flow rate 750 mL min^{-1}); absorbance measurements at 1385 nm.

Analytical performance of iHEART

In addition to the assessment for multivariate determination of hydrocarbon mixtures, the iHEART was evaluated regarding some other aspects of analytical importance, therefore attesting its feasibility for continuous monitoring of (petro)chemical processes, as well as for other applications, which require minute amounts of gaseous samples.

The total volume of the hiHWG gas cell is approx. 4.0 mL. In order to evaluate the response time of the sensor, nitrogen and pure methane were alternately flushed into the waveguide. From Fig. 7, the response time for the sensor is around 30 s for a flow rate of 280 mL min^{-1} , while the cleaning time is approximately the same for a nitrogen flow rate of 510 mL min^{-1} . Besides the rapid response time, these results indicate that a sample volume of approx. 140 mL is necessary for one measurement, thus rendering the iHEART sensor appropriate for analyses in scenarios only providing reduced sample volumes.

Conclusions

A novel heart-shaped substrate-integrated hollow waveguide (hiHWG) was integrated with a near infrared micro-spectrometer (μ NIR), providing a compact and robust system for sensing natural gases. The iHEART system, which makes use of the internal light source of the μ NIR spectrometer, is powered through the USB connector of a notebook, affording enough compactness for in field measurements. The performance of the iHEART system based on near-infrared micro-spectrometers was compared with a laboratory-based AOTF NIR spectrometer, thereby demonstrating its capability as an analytical tool for (petro)chemical process monitoring. In addition, owing to the short sensor response time and the small sample volume, the iHEART system is also suitable for other monitoring purposes that demand minute amounts of samples, such as in breath analysis of small animal models.

Acknowledgements

Financial support from CNPq (Project 407170/2013-8 – Optical Sensor Technologies for Environmental, Medical, and Process Analytics (OSTEMPA)) and INCTAA (CNPq 573894/2008-6 and FAPESP 2008/57808-1) is greatly acknowledged.

References

- 1 L. F. Capitán-Vallvey and A. J. Palma, *Anal. Chim. Acta*, 2011, **696**, 27–46.
- 2 A. Hardfield and J. Hajdu, *J. Appl. Crystallogr.*, 1993, **26**, 839–842.
- 3 D. Sorak, L. Herberholz, S. Iwascek, S. Altinpinar, F. Pfeifer and H. W. Siesler, *Appl. Spectrosc. Rev.*, 2012, **47**, 83–115.
- 4 M. B. Bueno Guerra, E. de Almeida, G. G. A. Carvalho, P. F. Souza, L. C. Nunes, D. S. Júnior and F. J. Krug, *J. Anal. At. Spectrom.*, 2014, **29**, 1667–1674.
- 5 E. Birkel and L. Rodriguez-Saona, *J. Am. Oil Chem. Soc.*, 2011, **88**, 1477–1483.
- 6 C. A. T. dos Santos, M. Lopo, R. N. M. J. Páscoa and J. A. Lopes, *Appl. Spectrosc.*, 2013, **67**, 1215–1233.
- 7 A. Gałuszka, Z. M. Migaszewski and J. Namieśnik, *Environ. Res.*, 2015, **140**, 593–603.
- 8 M. Alcalà, M. Blanco, D. Moyano, N. Broad, N. O'Brien, D. Friedrich, F. Pfeifer and H. Siesler, *J. Near Infrared Spectrosc.*, 2013, **21**, 445–457.
- 9 E. J. N. Marques, S. T. De Freitas, M. F. Pimentel and C. Pasquini, *Food Chem.*, 2016, **197**, 1207–1214.
- 10 E. M. Paiva, J. J. R. Rohwedder, C. Pasquini, M. F. Pimentel and C. F. Pereira, *Fuel*, 2015, **160**, 57–63.
- 11 O. M. D. Lutz, G. K. Bonn, B. M. Rode and C. W. Huck, *Anal. Chim. Acta*, 2014, **826**, 61–68.
- 12 J. J. R. Rohwedder, C. Pasquini, P. R. Fortes, I. M. Raimundo Jr., A. Wilk and B. Mizaikoff, *Analyst*, 2014, **139**, 3572–3576.
- 13 A. Wilk, J. C. Carter, M. Chrisp, A. M. Manuel, P. Mirkarimi, J. B. Alameda and B. Mizaikoff, *Anal. Chem.*, 2013, **85**, 11205–11210.
- 14 P. R. Fortes, A. Wilk, F. Seichter, M. Cajlakovic, S. Koestler, V. Ribishit, U. Wachter, J. Vogt, P. Radermacher, C. Carter, I. M. Raimundo, Jr. and B. Mizaikoff, *Proc. SPIE*, 2013, **8570**, 85700Q-1.
- 15 J. F. S. Petrucci, P. R. Fortes, V. Kokoric, A. Wilk, I. M. Raimundo, Jr., A. A. Cardoso and B. Mizaikoff, *Sci. Rep.*, 2013, **3**, 3174.
- 16 J. F. S. Petrucci, P. R. Fortes, V. Kokoric, A. Wilk, I. M. Raimundo, Jr., A. A. Cardoso and B. Mizaikoff, *Analyst*, 2014, **139**, 198–203.
- 17 M. M. C. Ferreira, *Quimiometria: Conceitos, Métodos e Aplicações*, Editora Unicamp, Campinas-SP, 2015.
- 18 P. Valderrama, J. W. B. Braga and R. J. Poppi, *J. Braz. Chem. Soc.*, 2007, **18**, 259–266.

